UDC 621.891 (043.3) DOI: 10.18372/0370-2197.2(107).20168

O. TAMARGAZIN, L. PRYIMAK, I. MORSHCH
State University «Kyiv Aviation Institute»

INFLUENCE OF THERMAL REGIME ON THE STRUCTURAL-PHASE STATE OF COATINGS BASED ON 11Р3АМФ2 STEEL

This study investigates the dependence of reinforcing particle distribution on thermal regimes within the carbide subsystem of coatings based on 11Р3АМФ2 steel, obtained through surfacing. The variations in the volume fraction of secondary carbides and residual austenite in the matrix of the deposited coating were analyzed as functions of the thermal cycle during weld surfacing. The composition of secondary carbides was compared to that of eutectic carbides. It was determined that an increase in residual austenite content enhances the wear resistance of the coatings due to the γ→α′-martensitic transformation and the presence of dispersed secondary carbides within the matrix grains. The highest concentration of dispersed secondary carbides was observed in the reinforced layer heated to temperatures in the range of 600-700 °C. The wear resistance of the obtained coatings was evaluated using quartz sand and electrocorundum abrasives.

Key words: *composite materials, structural-phase composition, serviceability, weld surfacing.*

Introduction. As demonstrated in [1], the development of multimodal structures in coatings based on 11Р3АМФ2 steel holds significant promise. These coatings exhibit a marked increase in abrasive wear resistance. However, further investigation was required to assess the positive contribution of the volume fraction of residual austenite and dispersed secondary carbides to abrasive wear resistance under varying abrasive hardness conditions. Without such studies, the application of these coatings in the restoration of friction pairs in highly loaded aviation components remains limited is too complicated one. The methodologies and equipment used in this study are detailed in [2].

Substrate temperature variations during deposition. Temperature measurements during electron beam deposition were conducted using a WRNK-131 (chromel-alumel) thermocouple, capable of measuring temperatures up to 1100 °C. The thermocouple was positioned 0.4-0.6 mm from the surface of the base metal onto which the coating was applied.

The weld surfacing process was performed in four passes, with each pass lasting 80 seconds, followed by a cooling period of 60-70 seconds. Figure 1 illustrates a representative curve of the base metal temperature variation during surfacing. Notably, the base metal underwent preliminary low-power electron beam treatment to refine its surface, resulting in a temperature increase from 45 to 115 °C as the base metal thickness varied from 50 to 5 mm.

As shown in Fig. 1, the base metal temperature increases with the number of passes, though the rate of temperature increase diminishes with each subsequent pass. Fig. 2 depicts the dependence of the maximum base metal temperature after four passes on the base metal thickness. Experiments revealed that for a 5 mm thick base metal, the temperature reached 830-840 °C, while for the maximum thickness of 50 mm, it did not exceed 400-420 °C.

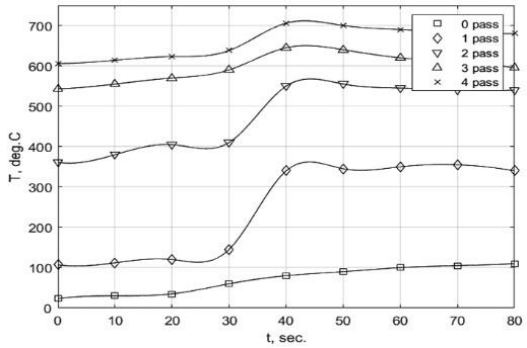

Fig. 1. Variation of base metal temperature with the number of electron beam passes for a base metal thickness of 5 mm

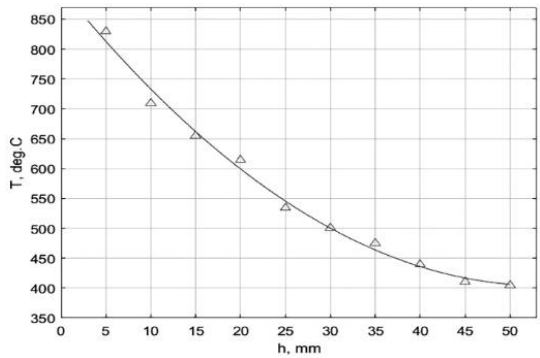

Fig. 2. Dependence of maximum base metal temperature after four passes on base metal thickness

Cooling of the experimental samples was conducted in a vacuum chamber. Representative cooling curves are presented in Fig.3. Analysis of these curves indicates that for a 5 mm thick base metal, the cooling time to 150 °C ranged from 1600 to 1700 seconds. For samples with a base metal thickness exceeding 20 mm, the cooling time to 200 °C was nearly constant, approximately 3200 seconds.

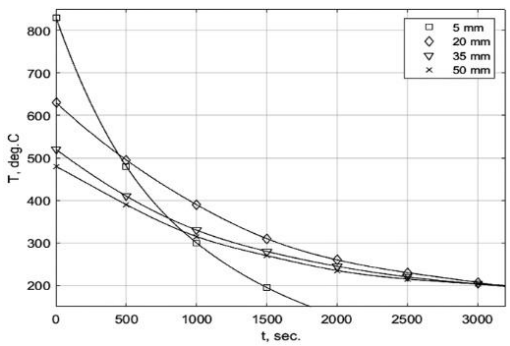

Fig. 3. Variation of cooling time for base metal samples after weld surfacing

Analysis of thermokinetic diagrams of supercooled austenite decomposition, as conducted in [3], identified a temperature range (830-500 °C) in which dispersed secondary carbides form in the austenitic matrix. Depending on the cooling rate post-deposition, austenite decomposition occurs via diffusional or martensitic mechanism.

Based on this, it was hypothesized that samples with base metal heated above 500 °C would exhibit the highest content of dispersed secondary carbides in the austenitic matrix. In this study, samples with base metal thicknesses up to 30 mm were heated above 500 °C.

Structural-phase state of coatings. Integral micro-X-ray spectral analysis (20 analyzed points) was performed on the investigated samples. The chemical composition of the deposited layer was determined as follows: Fe, 3.7% Cr, 2.4% V, 2.3% Mo, 2.1% W (wt. %). Combined analysis using optical microscopy, scanning electron microscopy, X-ray diffraction, and electron microscopy revealed that the reinforcing phase in the coatings consists of M_6C, M_2C, and VC carbides. Eutectic M_6C carbides, forming a network along grain boundaries of the solid solution (Fig. 4), had an average size of 3.4 μm and a volume fraction of approximately 4.1% (Fig. 5).

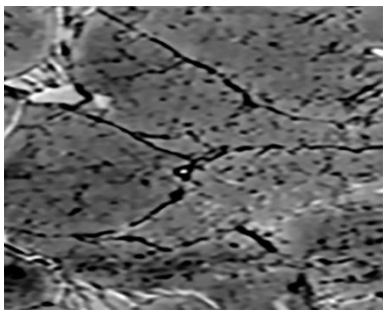

Fig. 4. Microstructure of the deposited surface, obtained via scanning electron microscopy for a sample with a 20 mm thick base metal

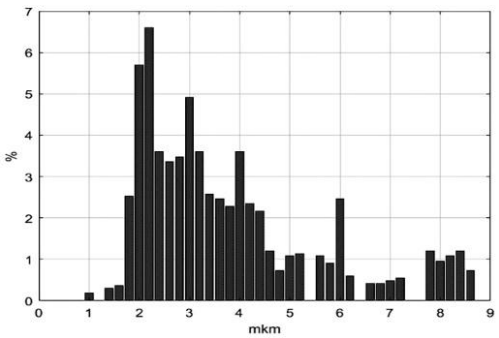

Fig. 5. Size distribution of eutectic carbides

The second morphological type of carbides identified was dispersed, elongated M_2C carbides. Their average size was 0.33 μm in the tangential direction and 1.27 μm in the radial direction. These M_2C carbides were located within the matrix grains and exhibited varying dispersity, as evidenced by distinct and diffuse patterns in microdiffraction images. Fig. 6 illustrates the variation in the volume fraction of dispersed secondary carbides with base metal thickness.

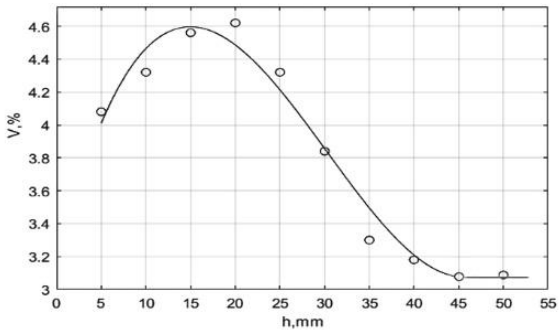

Fig. 6. Volume fraction of dispersed secondary carbides on base metal thickness-dependent

It was concluded that samples with base metal thicknesses up to 30 mm exhibited the highest volume fraction of dispersed secondary carbides (8.1%) in the reinforced layer. This is attributed to the samples being heated to 600-700 °C during weld surfacing, corresponding to the temperature range for secondary carbide precipitation [3].

Chemical analysis of the structural constituents of the deposited coatings was performed using energy-dispersive X-ray spectroscopy. This analysis revealed a significant reduction in vanadium content in M_2C secondary carbides compared to M_6C eutectic carbides. Transmission electron microscopy indicated that the dispersed secondary carbides were Mo_2C with an ordered hexagonal lattice

Vanadium carbide in the deposited layer was present as isolated, rounded particles, primarily located near M_6C eutectic carbides. Their average size was 0.7 μm, with a volume fraction not exceeding 1%.

As shown in Fig. 7, the matrix of the deposited layer exhibited a two-phase state consisting of martensite and residual austenite. Microdiffraction analysis revealed a disoriented grain-subgrain structure with high internal stresses. Ultrafine carbide phases were uniformly distributed within martensitic lamellae but could not be identified due to overlapping reflections with α-martensite.

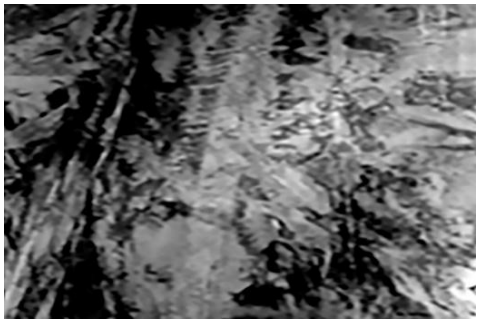

Fig.7. Microstructure of the matrix phase

The variation in martensite content within the matrix of the deposited coating is shown in Fig. 8.

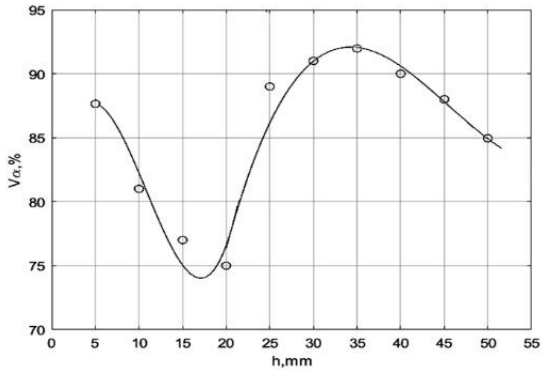

Fig.8. Variation of martensite content in the matrix of the deposited coating

This dependence exhibits a minimum, attributed to the varying heating temperatures of the samples, which depend on the base metal thickness. Thus, the structural-phase state of the reinforced layer, formed during multi-pass weld surfacing, varies in the quantitative ratio of the carbide and matrix subsystems depending on the base metal thickness.

In the carbide subsystem, a multimodal distribution of reinforcing particles was observed, categorized by size as follows: fine-grained M_6C eutectic carbides (3 μm), submicrocrystalline particles (0.6 μm), and elongated M_2C secondary carbides (~0.3 μm). The thermal cycle of surfacing significantly influenced the volume fraction of M_2C secondary carbides, which varied by a factor of 1.5 depending on the base metal thickness.

Additionally, the quantitative ratio of residual austenite to martensite in the reinforced layer varied with base metal thickness. The maximum residual austenite content did not exceed 25% and corresponded to the highest volume fraction of M_2C secondary carbides. An ultrafine carbide phase, uniformly distributed within martensitic lamellae, was also present in the coating.

Therefore, these structural changes in the deposited layer, driven by temperature, determine its tribological properties, particularly enhancing of abrasive wear resistance, as demonstrated in subsequent tests.

Investigation of the abrasive wear resistance of the samples. In addition to hardness, the wear resistance of high-speed steels is significantly influenced by the quantity, distribution, and size of carbides, as well as the structural state of the matrix and the ability of metastable austenite to undergo martensitic transformation under external loading [4].

The higher wear resistance of cast high-speed steels compared to deformed high-speed steels can be attributed to the presence of a framework of hard eutectic carbides along the grain boundaries of the solid solution. This framework is more effective under abrasive and oxidative wear conditions than structurally isolated carbide particles.

Dispersed carbide precipitates are essential for protecting the relatively soft matrix grains from abrasion. Studies on WC-Co bulk composites [5, 6] demonstrated that transitioning from a microcrystalline to a nanocrystalline carbide phase structure, at constant cobalt content, reduces the thickness of the intercarbide matrix layer, increasing hardness. This significantly enhances wear resistance under both abrasive wear and sliding friction conditions, resulting from smaller carbide grain sizes and

thinner intercarbide layers, which limit selective wear and subsequent carbide particle dislodgement.

The presence of networked precipitates along grain boundaries and ultrafine-grained carbides within the grain boundaries and solid solution volume in harded layer, differing significantly in size, enhances the wear resistance of the deposited coating.

The martensitic transformation of the metastable austenitic matrix under applied external loads also contributes to improved wear resistance [6]. Studies on the deformation and fracture behavior of composite materials indicate that the matrix phase plays a critical role in ensuring material plasticity. Enhanced plasticity is driven by the matrix's ability to relax stress concentrations, thereby transferring loads to carbide particles and inhibiting crack propagation during carbide fracture. This occurs through structural phase transformations in the matrix, enabling simultaneous atomic displacement over interatomic distances and the formation of a new crystalline structure under stress in small material volumes, such as thin intercarbide layers.

As shown in Fig. 9, a minimum in wear resistance is observed at approximately 81.5% martensite content. To the left of this minimum, the relative wear resistance coefficient increases due to a higher residual austenite content, which undergoes γ→α'-martensitic transformation under external loading. Additionally, networked precipitates along grain boundaries and ultrafine carbides within the solid solution volume reduce matrix extrusion from intercarbide spaces.

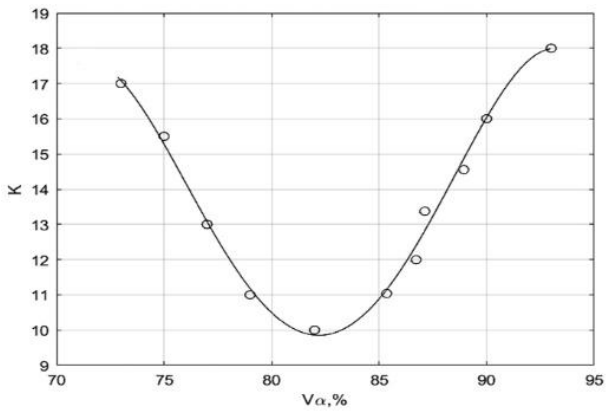

Fig.9. Variation of the relative wear resistance coefficient with the volume fraction of martensite in the matrix

The increase in wear resistance to the right of the minimum is associated with a higher total content of hard constituents (carbide particles and initial martensite) in the deposited coating. Tests under purely abrasive wear conditions using quartz sand showed increased wear resistance, though significant variability in wear coefficients was observed between samples. Conversely, under purely abrasive wear with electrocorundum, no significant increase in wear resistance was observed to the right of the minimum. Under impact-abrasive wear, the coating's wear resistance decreased due to substantial material loss from brittle fracture caused by extensive cracks propagation.

The influence of base metal thickness on the increase in α'-phase content in the near-surface volume of the deposited coating after wear testing is shown in Fig. 10.

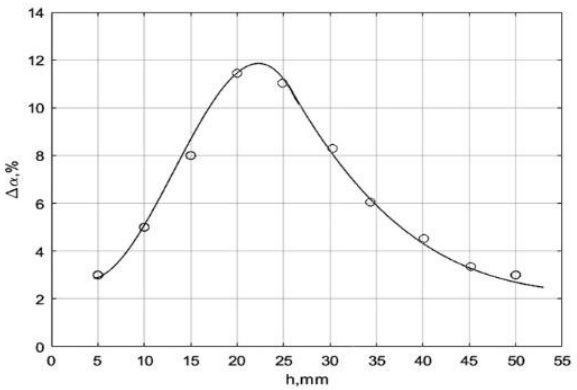

Fig. 10. Effect of base metal thickness on the increase in α'-phase content in the near-surface layer of the deposited coating

The graph demonstrates for base metal thicknesses of 10-20 mm, the deformation-induced martensite content in the near-surface volume increased from 4.5% to 12% after abrasive wear testing. Microhardness measurements and layer-by-layer X-ray structural analysis indicated that the depth of the layer undergoing γ→α'-transformation and substructural changes in the initial phases did not exceed 43 μm. These findings confirm that increased residual austenite content enhances coating wear resistance through γ→α'-martensitic transformation and the presence of dispersed secondary carbides within matrix grains.

Conclusions. This study demonstrates that, depending on the base metal thickness and the corresponding thermal regime during multi-pass weld surfacing of a reinforcing layer based on 11R3AMF2 steel, a multimodal distribution of reinforcing particles with varying sizes forms in the carbide subsystem. The volume fraction of secondary carbides and residual austenite in the matrix varies widely depending on the thermal cycle of surfacing. The vanadium content in secondary carbides was found to be reduced by nearly fourfold compared to eutectic carbides. Increased residual austenite content enhances the wear resistance of the deposited coating through γ→α'-martensitic transformation and the presence of dispersed secondary carbides within matrix grains. The highest concentration of dispersed secondary carbides was observed in the reinforced layer heated to 600-700 °C, corresponding to samples with base metal thicknesses up to 20 mm, where the secondary carbide volume fraction reached approximately 8%.

References

1. Tamargazin, O.; Pryimak, L.; Morshch, I. Substantiation of Expediency of Use of Tool High-Speed Cutting Steels as Coatings in Friction Units / Проблеми тертя та зношування, 2024, 1(102), С. 4-13, DOI: 10.18372/2310-5461.61.18515

2. Tamargazin, O.; Pryimak, L.; Morshch, I. Methodological Support for Research on the Feasibility of Using High-Speed Tool Steel as Coatings in Friction Units / Проблеми тертя та зношування, 2025, 1(106), С. 78-85, DOI: 10.18372/0370-2197.1(106).19827

3. Shuili Gong, Jianrong Liu, Guang Yang, Haiying Xu Electron Beam Wire Deposition Technology and Its Application, Springer, National Defense Industry Press, 2022, 312 pp.

4. Jimei, Xiao ed. Alloying phase and phase transformation (Second ed.), Beijing: Metallurgy industry Publisher, 2004

5. John F. Watts, John Wolstenholme an Introduction to Surface Analysis by XPS and AES, 2003, 224 pp.

6. Raghavan V. Physical Metallurgy: Principles and Practice, 2015, 260 pp.

Стаття надійшла до редакції 10.02.2025.

Oleksandr Anatoliyovych Tamargazin – Doctor of Technical Sciences, Professor, Professor of the Department of Airport Technologies, State University «Kyiv Aviation Institute», 1 Lubomyra Huzar Ave., Kyiv, Ukraine, 03058, https://orcid.org/0000-0002-9941-3600

Liudmyla Borysivna Pryimak – Candidate of Technical Sciences, Associate Professor, Associate Professor of the Department of Airport Technologies, State University «Kyiv Aviation Institute», 1 Lubomyra Huzar Ave., Kyiv, Ukraine, 03058, https://orcid.org/0000-0002-3354-9820

Illia Volodimirovich Morshch – postgraduate student of the Department of Airport Technologies, State University «Kyiv Aviation Institute», 1 Lubomyra Huzar Ave., Kyiv, Ukraine, 03058, https://orcid.org/0000-0002-8517-7536

О.А. ТАМАРГАЗІН, Л.Б. ПРИЙМАК, І.В. МОРЩ

ВПЛИВ ТЕМПЕРАТУРНОГО РЕЖИМУ НА СТРУКТУРНО-ФАЗОВИЙ СТАН ПОКРИТТІВ НА ОСНОВІ СТАЛИ 11Р3АМФ2

Розглянуто результати залежності розподілу зміцнювальних частинок від температурного режиму в карбідній підсистемі, отриманої при наплавленні шару на основі сталі 11Р3АМФ2. Проаналізовано зміни об'ємної частки вторинного карбіду і залишкового аустеніту матриці в покритті, що наплавляється в залежності від термічного циклу наплавлення. Досліджено склад вторинних карбідів у порівнянні з евтектичними карбідами. Визначено, що зі збільшенням кількості залишкового аустеніту в досліджуваному покритті, що наплавляється, їх зносостійкість підвищується за рахунок γ→α'-мартенситного перетворення, а також за рахунок наявності дисперсних вторинних карбідів в об'ємі зерен матриці. Найбільше дисперсних вторинних карбідів спостерігалося в зміцненому шарі, який нагрівався до температури в діапазоні 600-700 °С. Проведено дослідження отриманих покриттів на зносостійкість з використанням кварцового піску та електрокорунду.

Ключові слова: композиційні матеріали, структурно-фазовий склад, працездатність, наплавка

Список літератури

1. Tamargazin, O.; Pryimak, L.; Morshch, I. Substantiation of Expediency of Use of Tool High-Speed Cutting Steels as Coatings in Friction Units / Проблеми тертя та зношування, 2024, 1(102), С. 4-13, DOI: 10.18372/2310-5461.61.18515

2. Tamargazin, O.; Pryimak, L.; Morshch, I. Methodological Support for Research on the Feasibility of Using High-Speed Tool Steel as Coatings in Friction Units / Проблеми тертя та зношування, 2025, 1(106), С. 78-85, DOI: 10.18372/0370-2197.1(106).19827

3. Shuili Gong, Jianrong Liu, Guang Yang, Haiying Xu Electron Beam Wire Deposition Technology and Its Application, Springer, National Defense Industry Press, 2022, 312 pp.

4. Jimei, Xiao ed. Alloying phase and phase transformation (Second ed.), Beijing: Metallurgy industry Publisher, 2004

5. John F. Watts, John Wolstenholme an Introduction to Surface Analysis by XPS and AES, 2003, 224 pp.

6. Raghavan V. Physical Metallurgy: Principles and Practice, 2015, 260 pp.

Тамаргазін Олександр Анатолійович – докт. техн. наук, професор, професор кафедри технологій аеропортів ДНП «ДУ «КАІ», пр. Любомира Гузара, 1, м. Київ, Україна, 03058, https://orcid.org/0000-0002-9941-3600

Приймак Людмила Борисівна – канд. техн. наук, доцент, доцент кафедри технологій аеропортів ДНП «ДУ «КАІ», пр. Любомира Гузара, 1, м. Київ, Україна, 03058, https://orcid.org/0000-0002-3354-9820

Морщ Ілля Володимирович – аспірант кафедри технологій аеропортів ДНП «ДУ «КАІ», пр. Любомира Гузара, 1, м. Київ, Україна, 03058, https://orcid.org/0000-0002-8517-7536